Rectangular and radial region of interests on the edge of cylindrical phantom for spatial resolution measurement

Choirul Anam[1], Nazil Ainurrofik[1], Heri Sutanto[1], Ariij Naufal[1], Mohammad Haekal[2]
[1]Department of Physics, Faculty of Sciences and Mathematics, Diponegoro University, Semarang, Indonesia
[2]Department of Physics, Faculty of Science and Data Analytics, Institut Teknologi Sepuluh Nopember, Surabaya, Indonesia

Article Info

ABSTRACT

The purpose of this study was to evaluate the effect of rectangular region of interest (ROI) size on modulation transfer function (MTF), to develop the radial ROI, and to compare both ROIs performances for MTF measurement using a cylindrical polymethyl methacrylate (PMMA) phantom. The PMMA phantom used in this study was rotated 45°. Four rectangular ROIs and a radial ROI were created to measure the MTF value. The rectangular ROI sizes were 3×41, 21×41, 41×41, and 61×41 pixels; each was placed at upper phantom edge. The radial ROI's length was 41 pixels and placed at several points in phantom edge. The MTF calculation was automatically conducted using MATLAB. The MTFs from rectangular ROIs and radial ROI were then compared. The comparison of the MTF measurement was also conducted using three different filters. The MTF which used radial ROI was smoother than those of rectangular ROI for all filters. This indicated that radial ROI was more resistant to noise than rectangular ROI. Rectangular ROI with the 41×41 pixels had similar 50% and 10% MTF values with the radial ROI. The MTF value which was obtained using radial ROI is more accurate and robust than those obtained using rectangular ROI.

Corresponding Author:

Choirul Anam
Department of Physics, Faculty of Science and Mathematics, Diponegoro University
Street of Prof Soedarto, SH, Tembalang, Semarang 50275, Central Java, Indonesia
Email: anam@fisika.fsm.undip.ac.id

1. INTRODUCTION

The quality of computed tomography (CT) image needs to be maintained by conducting regular quality control (QC). Spatial resolution is one of the important parameters measured in QC, which was conducted in a metric of modulation transfer function (MTF). The MTF calculation is initially introduced by Judy [1], with the main purpose was to identify frequency domain response of imaging systems [2], [3]. MTF measurement was also used to characterize small structure [4], [5] and to compare the performance of imaging systems [6]. Thus, accurate MTF measurement is needed.

MTF can be measured using point, line and edge objects where the objects are spread and lead to the point spread function (PSF), line spread function (LSF), and edge spread function (ESF) [7], [8]. The MTF would then be obtained by applying Fourier transform to the LSF and PSF which would produce 1-dimensional (1D) and 2-dimensional (2D) MTF, respectively. Furthermore, MTF could also obtained by differentiating and applying Fourier transformation to the ESF [9]-[11].

Kayugawa *et al*. [12] conducted a study to find out an optimal size for square region of interest (ROI) used for calculating accurate and precise MTF using CatPhan 600 and a thin wire phantom. The results showed that the optimal sizes for square ROI were 50 pixels for FC10 filter, 38 pixels for FC50 filter, and 40 pixels for FC52 filter when using bead method. Optimal sizes for square ROI were 42 pixels for FC10 filter, 39 pixels

for FC50 filter and 44 pixels for FC52 filter when using wire method. Therefore, the size of the ROI used in the process of MTF calculation can affect the accuracy of the MTF. There are several phantoms used to practically measure MTF, such as CatPhan 600 [12], [13], ACR [14], [15], wire [16], [17] and AAPM CT performance phantom [18], [19]. In developing countries, those phantoms were only owned by few hospitals. Recently, there were studies that conducted MTF measurement using PMMA phantom [20]. Anam *et al.* [20] proposed a MTF measurement using the PMMA phantom. The PMMA phantom was rotated 45 degrees (clockwise/counter-clockwise) to avoid the ionization pencil holes. This MTF measurement was compared with using wire phantoms. The difference of MTF measurement using the upper of edge PMMA and wire phantoms was only within ± 4% [20]. However, in that study, a square ROI at circular edge of phantom was used and it may decrease the MTF value because circular phantom edge is linearly averaged in x-axis direction. Therefore, in the current study, the effect of rectangular ROI size on MTF measurement will be analyzed. We hypothesize that decreasing ROI size will yield a more accurate MTF. However, small ROI size may be susceptible to the noise. In addition, we will develop radial ROI which will be placed at several point in edge of PMMA phantom and compare the resulted MTF to those from rectangular ROIs.

2. METHOD

2.1. ROI determination

The head PMMA phantom with a diameter of 16 cm was used in this study. The phantom was scanned with a Toshiba Alexion-4 CT scanner with three different filters: FC13, FC30, and FC52. The parameters of scanning were field of view (FOV) of 20 cm, 120 kVp, 100 mA, rotation time of 1 s, slice thickness of 2 mm, and using axial mode. In this study, the phantom was rotated 45 degrees. In the phantom, there are five ionization chamber pencil holes. Figure 1 shows the position of the holes in each image, with filter FC13 (Figure 1(a)), FC30 (Figure 1(b)), and FC52 (Figure 1(c)).

In this study, the algorithm from Droege and Morin [19] was improved using MATLAB software. Previously, Anam *et al.* [20] used 41×41 pixels ROI and the measurement was performed automatically. Figure 2 shows various ROI size used in this study. The current study used four sizes of rectangular ROIs: 3×41 (Figure 2(a)), 21×41 (Figure 2(b)), 41×41 (Figure 2(c)), and 61×41 pixels (Figure 2(d)). The radial ROI was automatically measured along the edge of phantom (Figure 2(e)). Each line of radial ROI had length of 41 pixels.

The radial ROI was formed with four steps. First, the phantom image was segmented. Second, the center of the image was determined. Third, a line which passed through the edge of phantom image perpendicularly was yielded. The last, ROIs one by one along the edge of phantom image in 35 to 55 degrees except in the ionization pencil holes were formed.

2.2. MTF measurement

MTF measurement was performed automatically, which was started by taking all profiles of the ROIs. For rectangular ROIs, the value of each pixel along the x-axis was averaged to yield the ESF. For radial ROIs, the profile of each ROI was taken and then averaged to yield single averaged profile of ESF. Each ESF was interpolated to place four additional data. The interpolated ESFs were then differentiated, zeroed, and normalized to yield the line spread function (LSF) curve. Fourier transform was then applied to the LSF curve in order to obtain the MTF curve. The value of MTF at 10% and 50% were automatically determined. The steps of MTF determination using radial ROI could be seen in the Figure 3.

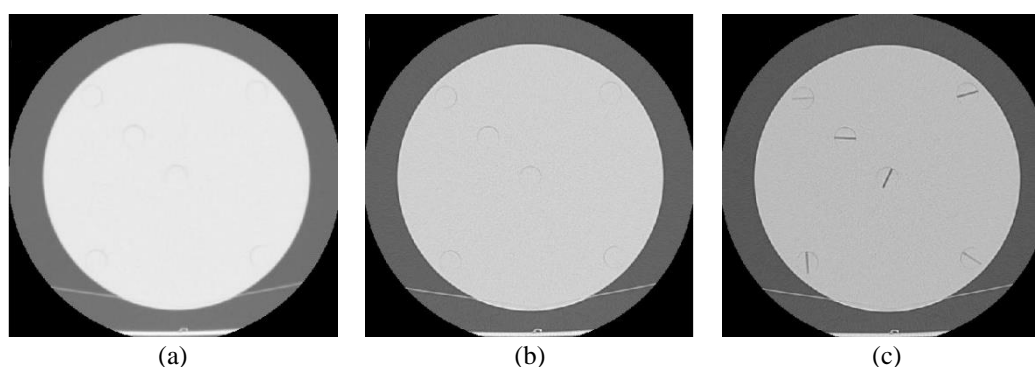|		
(a)	(b)	(c)

Figure 1. Images of phantom with different filters were rotated 45 degrees; Filter (a) FC13, (b) FC30, and (c) FC52
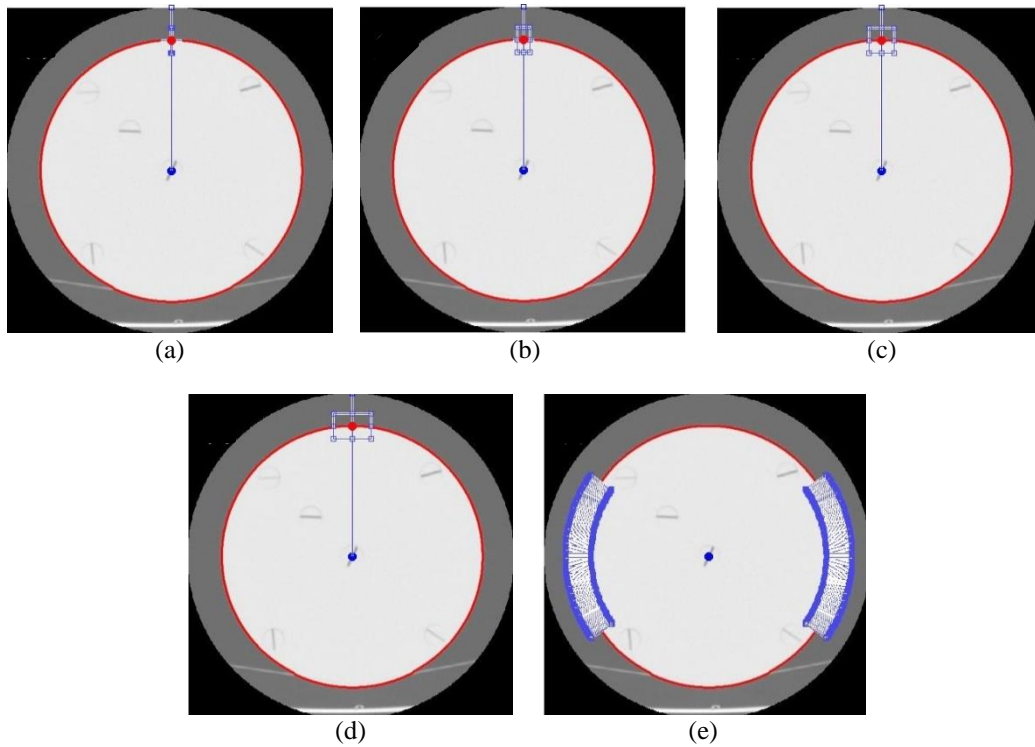
Figure 2. The different ROIs were used for measuring MTF on head PMMA phantom. Four rectangular ROI sizes are (a) 3×41 pixels, (b) 21×41 pixels, (c) 41×41 pixels, (d) 61×41 pixels, and (e) radial ROI
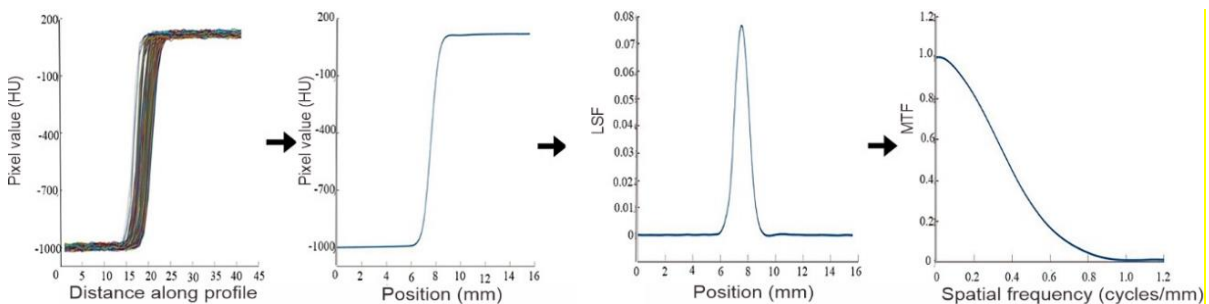

Figure 3. The steps of MTF determination using radial ROI

3.   RESULTS AND DISCUSSION

Figure 4 shows the results of image filtered with FC13 from all ROIs, with it's ESF (Figure 4(a)), LSF (Figure 4(b)), and MTF (Figure 4(c)). The curves of the ESF is shown to be overlapping with one another, indicating that all MTFs are comparable. However, the ESF curve of ROI size of 3×41 pixels is shown to be more fluctuating due to the image noise, as predicted. These lead to a more fluctuating LSF curve because of the differentiation process. As a result, the MTF curve produced from this ROI also became more fluctuated. On the other hand, the measurement which used ROI size of 61×41 pixels produce the lowest peak at LSF curve. The MTF curve produced by this ROI was also decreasing faster than the other, indicating that it produces lower spatial resolution, as predicted. The 10% and 50% MTF values are tabulated in the Table 1.

Figure 5 shows the results of image filtered with FC30 from all ROIs, with it's ESF (Figure 5(a)), LSF (Figure 5(b)), and MTF (Figure 5(c)). It can be seen that all ESF curves for radial and all rectangular ROI sizes have similar form, except for 3×41 ROI. Both tails of the LSF curves for all ROIs were also shown to have negative peaks. In the MTF curve, radial ROI has the highest peak of ± 1.2. The MTF curve of 3×41 rectangular ROI obtained by using this filter was also shown to be fluctuating. The 10% and 50% MTF values are tabulated in the Table 2.
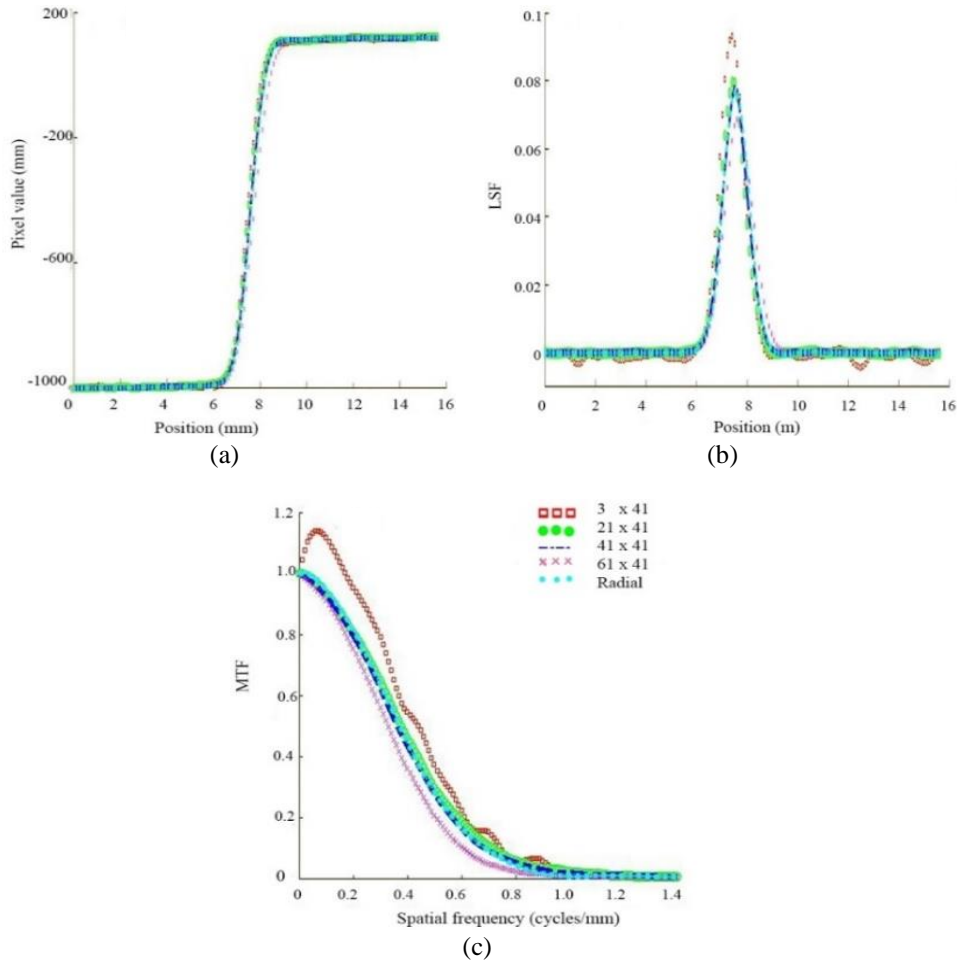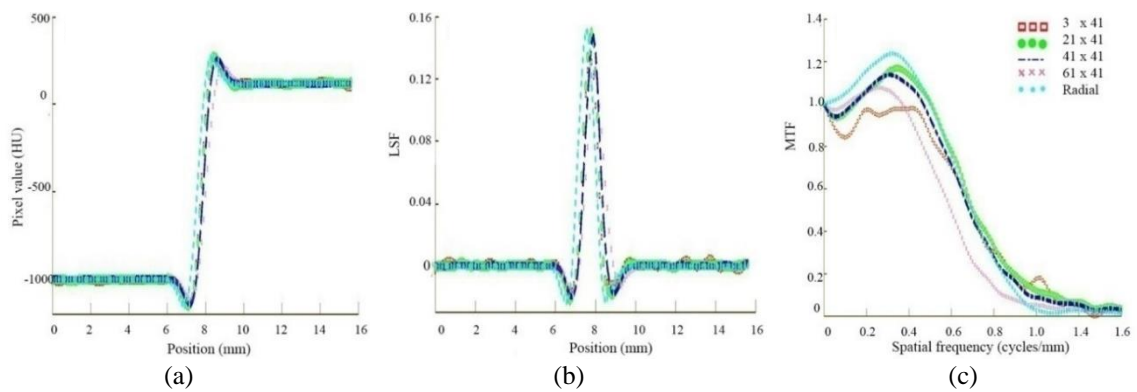
(a)

(b)

(c)

Figure 4. The comparison of (a) ESF, (b) LSF, and (c) MTF using FC13 filter for rectangular ROI sizes of 3×41, 21×41, 41×41, 61×41 pixels, and radial ROI

Table 1. The values of 10% and 50% MTFs for the rectangular ROIs and radial ROIs using FC13 filter

ROI types	ROI size (pixels)	Spatial resolution (cycles/mm)	
		MTF 10%	MTF 50%
Rectangular	3×41	0.71±0.05	0.38±0.04
	21×41	0.71±0.01	0.38±0.01
	41×41	0.69±0.01	0.37±0.00
	61×41	0.62±0.01	0.33±0.00
Radial	1×41	0.69±0.00	0.37±0.00

(a)

(b)

(c)

Figure 5. The comparison of (a) ESF, (b) LSF, and (c) MTF using FC30 filter for rectangular ROI sizes of 3×41, 21×41, 41×41, 61×41 pixels, and radial ROI

Table 2. The values of 10% and 50% MTFs for the rectangular ROIs and radial ROIs using FC30 filter

ROI types	ROI size (pixels)	Spatial resolution (cycles/mm)	
		MTF 10%	MTF 50%
Rectangular	3×41	1.11±0.07	0.66±0.22
	21×41	1.07±0.02	0.72±0.02
	41×41	1.01±0.03	0.70±0.01
	61×41	0.86±0.03	0.60±0.01
Radial	1×41	0.93±0.00	0.70±0.01

Figure 6 shows the results of image filtered with FC52 from all ROIs, with it's ESF (Figure 6(a)), LSF (Figure 6(b)), and MTF (Figure 6(c)). In the ESF, LSF, and MTF curves, the rectangular ROI size of the 3×41 pixels was also shown to have large fluctuation. The MTF of 61×41 pixels produces lowest spatial resolution. The 10% and 50% MTF are tabulated in the Table 3.
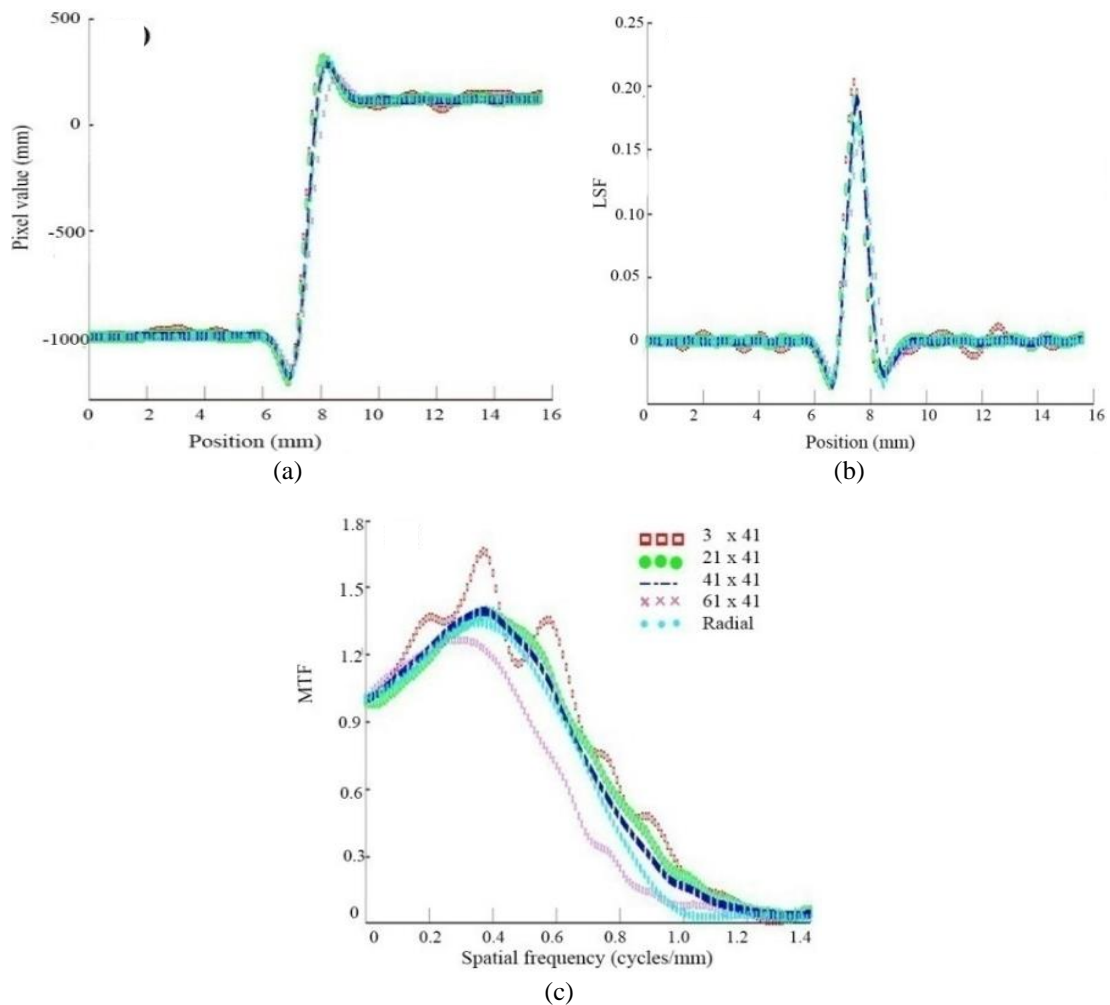

Figure 6. The comparison of (a) ESF, (b) LSF, and (c) MTF using FC52 filter for rectangular ROI size of 3×41, 21×41, 41×41, 61×41 pixels, and radial ROI

Table 3. The values of 10% and 50% MTFs for the rectangular ROIs and radial ROIs using FC52 filter

ROI types	ROI size (pixels)	Spatial resolution (cycles/mm)	
		MTF 10%	MTF 50%
Rectangular	3×41	1.55±0.64	0.87±0.12
	21×41	1.11±0.03	0.81±0.03
	41×41	1.07±0.02	0.77±0.01
	61×41	0.94±0.02	0.65±0.01
Radial	1×41	0.95±0.01	0.76±0.00

Figure 7 shows the MTF comparison for 41×41 pixels and radial ROI for all filters, with FC13 shown in Figure 7(a), FC30 in Figure 7(b), and FC52 in Figure 7(c). The curves which was using FC13 filter were shown to coincide. The value of 10% and 50% MTF for radial ROI are slightly higher than 41×41 pixels of rectangular ROI. However, MTF curves using FC30 filter for radial ROI is smoother than 41×41 pixels of rectangular ROI, where 50% MTF of radial ROI is slightly higher than 41×41 rectangular ROI but 10% MTF of radial ROI is lower than 41 × 41 rectangular ROI. MTF curves using FC52 filter for 41×41 rectangular ROI is slightly higher than radial ROI, but the overall curve of radial ROI is slightly smoother than 41×41 rectangular ROI. The 10% and 50% MTFs as shown in Table 4.
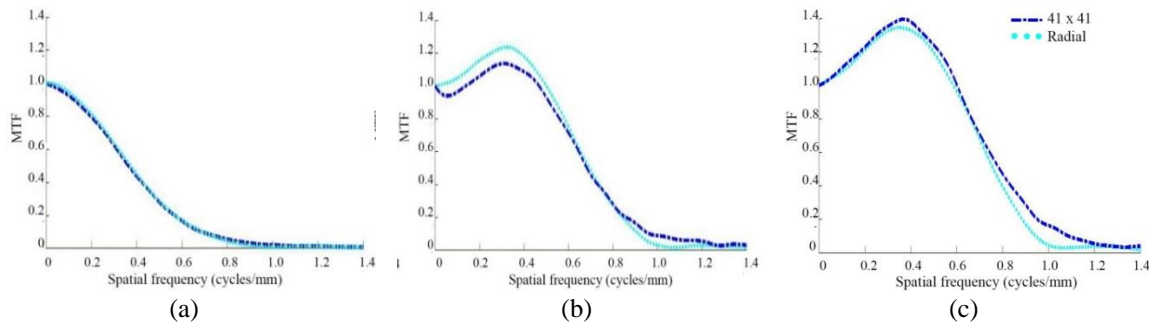
Figure 7. The MTF comparisons for rectangular ROI of 41×41 pixels and radial ROI using (a) FC13,
(b) FC30, and (c) FC52 filters

Table 4. The values of 10% and 50% MTFs for the 41×41 pixels of rectangular ROI and radial ROIs using FC13, FC30, and FC52 filters

ROI type	Spatial resolution (cycles/mm)					
	FC13		FC30		FC52	
	MTF 10%	MTF 50%	MTF 10%	MTF 50%	MTF 10%	MTF 50%
Rectangular (41×41)	0.69±0.01	0.37±0.00	1.01±0.03	0.70±0.01	1.07±0.02	0.77±0.01
Radial	0.69±0.00	0.37±0.00	0.93±0.00	0.70±0.01	0.95±0.01	0.76±0.00

This study developed the previous algorithm for automated MTF calculation on head PMMA phantom [20]. In the current study, 3 filters were investigated and produce different spatial resolution. The size and shape of the ROI were also shown to affect the accuracy of the MTF. Radial ROI has many lines of ROI and they can be used as additional representation of ESF and to decrease error due to noise [21]-[23]. The ESFs of the radial ROIs are averaged to produce single ESF [24].

The MTF curves from rectangular ROIs and radial ROI using FC13 filter were coinciding with each other, indicating that the MTFs are comparable. The rectangular ROI sizes of 3×41 pixels and 61×41 pixels for all filters are slightly different. The ROI size of 3×41 pixels has greater fluctuation than those with wider ROIs. The decrease of the ROI size resulted in less number of data points used to calculate the MTF. The smaller number of data is more affected by image noise [25]. Larger noise caused the MTF to have more fluctuations [22]. Fewer data can produce bias error caused by noise. Whereas, the rectangular ROI size of 61×41 pixels leads to lower spatial resolution for all filters due to the curved edge within the ROI is linearly averaged. This indicates that wider ROI will lead to lower spatial resolution. 10% and 50% MTF values using rectangular ROI sizes of 41×41 pixels, however, were similar to the radial MTF values for all filters. The radial ROI was created from several points in phantom edge [24]. The radial ROI for various filters was more resistant to noise due to many lines which were used for MTF calculation. Therefore, it can be used to accurately measure MTF on PMMA phantom which has circular edge.

The radial ROI method is accurate as long as the spatial resolution of the CT does not pass the Nyquist frequency. The Nyquist frequency of this imaging condition is 1.28 mm^{-1}. It can be seen from Figure 7(c), that the MTF which was using radial ROI dropped faster than those which used rectangular ROI because the frequency was close to the Nyquist frequency. If the spatial resolution of the CT system is greater that Nyquist frequency, smaller FOV should be used. However, that condition will cause the image to be truncated. Therefore, the MTF measurement using radial ROI requires alternative approach, such as using PMMA phantom with diameter of 8 cm and/or scanned with FOV of 12 cm or less. The 16 cm head PMMA phantom scanned with 24 cm FOV can also yield oversampling MTF using rectangular ROI method, if shifting and rebinning data approach are applied [25]. These approaches will be investigated in the future study.

4. CONCLUSION

The comparison of radial and rectangular ROIs has been successfully conducted. The results of this study show that the size of rectangular ROI affects accuracy of the MTF. It is found that MTF values of rectangular ROI with size of 41×41 pixels close to those from the radial ROI. Therefore, the optimal rectangular ROI size for MTF measurement using edge of PMMA phantom is 41×41 pixels. Radial ROI can be used to accurately measure MTF on PMMA phantom which has circular edge as long as the spatial resolution of the CT system does not pass the Nyquist frequency.

ACKNOWLEDGEMENTS

REFERENCES

[1]   P. F. Judy, "The line spread function and modulation transfer function of a computed tomographic scanner," *Medical Physics*, vol. 3, no. 4, pp. 233–236, Jul. 1976, doi: 10.1118/1.594283.
[2]   E. L. Nickoloff and R. Riley, "A simplified approach for modulation transfer function determinations in computed tomography," *Medical Physics*, vol. 12, no. 4, pp. 437–442, Jul. 1985, doi: 10.1118/1.595706.
[3]   K. Rossmann, "Point spread-function, line spread-function, and modulation transfer function. Tools for the study of imaging systems," *Radiology*, vol. 93, no. 2, pp. 257–272, Aug. 1969, doi: 10.1148/93.2.257.
[4]   S. Prevrhal, J. C. Fox, J. A. Shepherd, and H. K. Genant, "Accuracy of CT-based thickness measurement of thin structures: Modeling of limited spatial resolution in all three dimensions," *Medical Physics*, vol. 30, no. 1, pp. 1–8, Dec. 2003, doi: 10.1118/1.1521940.
[5]   M. Ohkubo, S. Wada, M. Kunii, T. Matsumoto, and K. Nishizawa, "Imaging of small spherical structures in CT: Simulation study using measured point spread function," *Medical and Biological Engineering and Computing*, vol. 46, no. 3, pp. 273–282, Mar. 2008, doi: 10.1007/s11517-007-0283-x.
[6]   H. H. Barrett and W. Swindell, *Radiological imaging: the theory of image formation, detection, and processing*. Elsevier, 2012, doi: 10.1016/C2009-0-02376-9.
[7]   B. K. Reid, "Signal and noise in modulation transfer functiom determinations using the slit, wire, and edge techniques," *Medical Physics*, vol. 19, no. 4, pp. 1037–1044, Jul. 1992, doi: 10.1118/1.596821.
[8]   P. B. Greer and T. Van Doorn, "Evaluation of an algorithm for the assessment of the MTF using an edge method," *Medical Physics*, vol. 27, no. 9, pp. 2048–2059, Sep. 2000, doi: 10.1118/1.1288682.
[9]   S. Maruyama, "Assessment of uncertainty depending on various conditions in modulation transfer function calculation using the edge method," *Journal of Medical Physics*, vol. 46, no. 3, pp. 221–227, 2021, doi: 10.4103/jmp.JMP_36_21.
[10]   C. Anam, F. Haryanto, R. Widita, I. Arif, and G. Dougherty, "An investigation of spatial resolution and noise in reconstructed CT images using iterative reconstruction (IR) and filtered back-projection (FBP)," *Journal of Physics: Conference Series*, vol. 1127, no. 1, p. 012016, Jan. 2019, doi: 10.1088/1742-6596/1127/1/012016.
[11]   M. Ohkubo, S. Wada, T. Matsumoto, and K. Nishizawa, "An effective method to verify line and point spread functions measured in computed tomography," *Medical Physics*, vol. 33, no. 8, pp. 2757–2764, Jul. 2006, doi: 10.1118/1.2214168.
[12]   A. Kayugawa, M. Ohkubo, and S. Wada, "Accurate determination of ct point-spread-function with high precision," *Journal of Applied Clinical Medical Physics*, vol. 14, no. 4, pp. 216–226, Jul. 2013, doi: 10.1120/jacmp.v14i4.3905.
[13]   C. T. Dodge *et al.*, "Performance evaluation of iterative reconstruction algorithms for achieving CT radiation dose reduction - A phantom study," *Journal of Applied Clinical Medical Physics*, vol. 17, no. 2, pp. 511–531, Mar. 2016, doi: 10.1120/jacmp.v17i2.5709.
[14]   S. N. Friedman, G. S. K. Fung, J. H. Siewerdsen, and B. M. W. Tsui, "A simple approach to measure computed tomography (CT) modulation transfer function (MTF) and noise-power spectrum (NPS) using the American College of Radiology (ACR) accreditation phantom," *Medical Physics*, vol. 40, no. 5, 2013, doi: 10.1118/1.4800795.
[15]   S. Richard, D. B. Husarik, G. Yadava, S. N. Murphy, and E. Samei, "Towards task-based assessment of CT performance: System and object MTF across different reconstruction algorithms," *Medical Physics*, vol. 39, no. 7, pp. 4115–4122, Jun. 2012, doi: 10.1118/1.4725171.
[16]   A. L. C. Kwan, J. M. Boone, K. Yang, and S. Y. Huang, "Evaluation of the spatial resolution characteristics of a cone-beam breast CT scanner," *Medical Physics*, vol. 34, no. 1, pp. 275–281, Dec. 2007, doi: 10.1118/1.2400830.
[17]   C. Anam *et al.*, "Automated MTF measurement in CT images with a simple wire phantom," *Polish Journal of Medical Physics and Engineering*, vol. 25, no. 3, pp. 179–187, Sep. 2019, doi: 10.2478/pjmpe-2019-0024.
[18]   N. J. Schneiders and S. C. Bushong, "Computer assisted MTF determination in CT," *Medical Physics*, vol. 7, no. 1, pp. 76–78, Jan. 1980, doi: 10.1118/1.594769.
[19]   R. T. Droege and R. L. Morin, "A practical method to measure the MTF of CT scanners," *Medical Physics*, vol. 9, no. 5, pp. 758–760, 1982.
[20]   C. Anam, T. Fujibuchi, W. S. Budi, F. Haryanto, and G. Dougherty, "An algorithm for automated modulation transfer function measurement using an edge of a PMMA phantom: Impact of field of view on spatial resolution of CT images," *Journal of Applied Clinical Medical Physics*, vol. 19, no. 6, pp. 244–252, Nov. 2018, doi: 10.1002/acm2.12476.
[21]   A. González-López, "Effect of noise on MTF calculations using different phantoms," *Medical Physics*, vol. 45, no. 5, pp. 1889–1898, May 2018, doi: 10.1002/mp.12847.
[22]   S. Mori *et al.*, "Physical performance evaluation of a 256-slice CT-scanner for four-dimensional imaging," *Medical Physics*, vol. 31, no. 6, pp. 1348–1356, May 2004, doi: 10.1118/1.1747758.
[23]   E. Buhr, S. Günther-Kohfahl, and U. Neitzel, "Accuracy of a simple method for deriving the presampled modulation transfer function of a digital radiographic system from an edge image," *Medical Physics*, vol. 30, no. 9, pp. 2323–2331, Aug. 2003, doi: 10.1118/1.1598673.
[24]   J. M. Boone, "Determination of the presampled MTF in computed tomography," *Medical Physics*, vol. 28, no. 3, pp. 356–360, Mar. 2001, doi: 10.1118/1.1350438.

[25]   I. Mori and Y. MacHida, "Deriving the modulation transfer function of CT from extremely noisy edge profiles," *Radiological Physics and Technology*, vol. 2, no. 1, pp. 22–32, Jan. 2009, doi: 10.1007/s12194-008-0039-9.

BIOGRAPHIES OF AUTHORS

Dr. Choirul Anam completed his Ph.D. in physics department, Bandung Institute of Technology (ITB). He received master degree from University of Indonesia (UI) and the B.Sc. degree from Diponegoro University (UNDIP). He is currently working as a lecturer and researcher at the UNDIP. His research interests are medical image processing and dosimetry for diagnostic radiology, particularly in CT. He has authored and co-authored over 150 papers. One of his papers published in the Journal of Applied Clinical Medical Physics (JACMP) had been awarded as the best medical imaging physics article in 2016. He was also recognised as an outstanding reviewer for the physics in medicine and biology (PMB) in 2018 and for the biomedical physics and engineering express (BPEX) in 2019. He is developer of two software, i.e. IndoseCT (for calculating and managing radiation dose of CT) and IndoQCT (for measuring CT image quality). He can be contacted at email: anam@fisika.fsm.undip.ac.id.

Nazil Ainurrofik is a graduate student of the physics master's program at Diponegoro University. Her research interest is CT image quality using MTF calculation. She can be contacted at email: nazilainurrofik1996@gmail.com.

Prof. Heri Sutanto is a lecturer in materials physics at Diponegoro University. His expertise is thin films, nanomaterials, and medical materials. He can be contacted at email: herisutanto@live.undip.ac.id.

Ariij Naufal is a graduate student of the physics master's program at Diponegoro University. He is the developer of IndoQCT. He can be contacted at email: ariij.2019@fisika.fsm.undip.ac.id.

Mohammad Haekal, Ph.D. is a lecturer at department of physics, Institut Teknologi Sepuluh Nopember. He completed his Ph.D. at Kyushu University, Japan. He can be contacted at email: haekal@its.ac.id.